Biophysical Journal Volume 71 October 1996 2222–2226

Scanning Force Microscopy Reveals Ellipsoid Shape of Chicken Erythrocyte Nucleosomes

Wolfgang Fritzsche and Eric Henderson
Iowa State University, Department of Zoology and Genetics, Ames, Iowa 50011 USA

ABSTRACT Scanning force microscopy was used to investigate the conformation of hypotonic spread chicken erythrocyte nucleosomes. Nucleosomal chains were prepared in low-salt conditions and fixed before centrifugation onto glass coverslips and air drying. The images of single nucleosomes were isolated by image processing, and the height and geometry of the resulting three-dimensional structures were investigated. An average nucleosome height of 4.2 ± 1.1 nm was determined. A virtual cross section at half-maximum height of the nucleosome structure was used for a characterization of the nucleosome geometry. The shape of this cross section was best described by an ellipse with an aspect ratio (major/minor axis) of ~1.30.

INTRODUCTION

The DNA in eukaryotic cells is folded in a hierarchical series of stages. The first step is formation of a complex of a histone protein octamer with approximately 146 bp of DNA, which is known as a nucleosome (Van Holde, 1988). Structure determination of nucleosomes based on x-ray crystallography yielded a disklike structure 5.5 nm thick with a diameter of 11 nm (Richmond et al., 1984). The structure of nucleosomes exhibits changes with ionic strength (Libertini and Small, 1982) and transcriptional activity (Sterner et al., 1987). A direct correlation between the level of histone H4 hyperacetylation and the extent of elongation of the nucleosomal shape was demonstrated by electron spectroscopic imaging of HeLa cells and chicken erythrocytes (Oliva et al., 1990). That study also demonstrated the salt dependence of the elongation; at higher Mg^{2+} concentrations the elongation differences due to hyperacetylation disappeared. Electron spectroscopic imaging combined with reconstruction algorithms yielded a shape of an ellipsoid ~10 nm in length and ~9 nm in diameter for calf thymus nucleosomal cores (Harauz and Ottensmeyer, 1984). Conformational study of nucleosomes by principal component analysis of their electron micrographs resulted in ellipsoid nucleosomal shapes with axis lengths of 14.1 and 10.5 nm (calf thymus) or 13.3 and 11.5 nm (HeLa) (Zabal et al., 1993).

In this study we use scanning force microscopy (SFM) for the structural analysis of nucleosomes. This microscopical technique elucidates the three-dimensional structure of biomolecules with nanometer resolution (for reviews see Bustamante et al., 1994; Hansma and Hoh, 1994) and has been applied to chromatin investigations (for reviews see Fritzsche et al., 1995b; Lyubchenko et al., 1995). SFM studies of reconstituted nucleosomes (Allen et al., 1993), hypotonic spread chicken erythrocyte nucleosomes (Fritzsche et al., 1994), and isolated nucleosomes from rDNA chromatin (Martin et al., 1995) have been reported.

We used scanning force micrographs for conformational characterization of the nucleosomes. This approach is based upon the extraction of cross sections of nucleosomes at half-maximum height and their geometrical description. The use of ratios between major and minor ellipse axes minimizes the influence of the broadening effect of the tip for the assumed case of a spherical tip.

MATERIALS AND METHODS

Nucleosome preparation

Chicken erythrocyte nucleosomes were prepared by isotonic lysis at pH 9 before centrifugation through a glucose/formaldehyde cushion onto glass coverslips (Trendelenburg and Puvion-Dutilleul, 1987). One hundred microliters of fresh heparinized chicken blood was washed in 5:1 medium (83 mM KCl, 17 mM NaCl, 10 mM Tris-HCl, adjusted to pH 7.4), resuspended in pH 9 water (distilled water adjusted to pH 9.0 using 0.01 M borate buffer; Merck), and homogenized by 10 gentle strokes in a Dounce homogenizer. The solution was diluted with pH 9 water until the brown color of the solution was hardly visible.

Perspex (Plexiglas) blocks with four centrifugation chambers (modified after Trendelenburg and Puvion-Dutilleul, 1987) were equipped with coverslips and filled with a 0.1 M sucrose/1% formaldehyde solution (adjusted to pH 8.7). The chambers were overlayed with 100 μl of the erythrocyte solution (in pH 9 water) and closed with rectangular coverslips. After centrifugation at 3000 × g for 30 min, the coverslips were removed and washed in pH 9 water before rinsing in Kodak Photoflow (4% aqueous solution adjusted to pH 8.6) and air drying.

Scanning force microscopy

Scanning was in contact mode under ambient conditions with a NanoScope III (Digital Instruments (DI), Santa Barbara, CA) equipped with a J-scanner with a 130 × 130 × 5 (x, y, z)-μm scan range and Si tips (Ultralever; Park Scientific Instruments, Sunnyvale, CA) with a tip radius of ~5 nm and a cantilever force constant of ~0.03 N/m. All nucleosome structures were imaged during one imaging session with the same tip.

Image processing

NanoScope screen files (8 bit) were imported as TIFF files into National Institutes of Health Image (National Institutes of Health, Bethesda, MD).

Received for publication 1 May 1996 and in final form 19 July 1996.

Address reprint requests to Dr. Eric Henderson, 2112 Molecular Biology Bldg., Iowa State University, Ames, IA 50011. Tel./Fax: 515-294-2876; E-mail: telomere@iastate.edu.

0006-3495/96/10/2222/05 $2.00

The images were inspected, and only nucleosomes that were isolated (e.g., not touching neighboring nucleosomes) but aligned in a "beads-on-a-string" pattern were chosen for further processing. This selection should ensure the use of mainly intact nucleosomes.

Although a lateral and height calibration was possible, all of the image-processing steps were based on pixel counts rather than nanometers, to simplify calculations and avoid rounding errors. Finally, the results were converted to nanometers.

A threshold just above the highest substrate (background) features was chosen to isolate the nucleosome structures before a subtraction of these isolated structures for further processing (Fig. 1c; Fritzsche and Henderson, 1996b). The resulting holes in the background were extended by a dilation (coefficient of 3; Russ, 1992) to remove edge artifacts, which were visible as a region of larger height values sourounding the holes. The dilation was repeated until all regions higher than the adjacent background were removed. Now the average pixel value of the remaining pixels was calculated and used as the average background level. The difference between the threshold and the average background yielded 1.3 nm.

The maximum height of a given nucleosome was the difference between the highest height value in the structure and the average background level.

For the determination of the nucleosome shape and width, the cross section at half-maximum height was chosen, and the area and perimeter of the section plane were determined. Furthermore, the length and orientation of the major and minor axis of the best fit ellipse of this plane were measured and used for shape characterization (Fig. 1 *c*).

RESULTS AND DISCUSSION

The scanning force microscope revealed the typical appearance of nucleosomal chains as described previously by electron microscopy (EM) (e.g., Zentgraf et al., 1980) or SFM investigations (Fritzsche et al., 1994, 1995a) of similarly prepared samples. A "beads-on-a-string" pattern is created by nucleosomal cores connected by the linker DNA, with center-to-center distances of ~30 nm (Fig. 1 *a*). The observed height depends upon the orientation of the adsorbed nucleosomes. The flat orientation should be clearly preferred during adsorption because of energetic constraints, and the flexibility of the extended nucleosomal chain due to the linker DNA gives the nucleosomes enough freedom of movement to reach this favorable conformation. Moreover, the surface tension occurring during air drying would probably flatten other orientations (e.g., standing on the edges). Nucleosome structures were selected before isolation by image processing. Determination of the nucleosome height for the selected structures yielded 4.2 ± 1.1 nm (Fig. 1 *b*). The distribution shows no sign of multiple maxima, therefore suggesting the inclusion of a single conformation with a defined height. The measured height refined the value of ~4.5 nm from the preliminary investigation of this sample (Fritzsche et al., 1994) and is lower than that derived from other SFM investigations of nucleosome heights of reconstituted samples (5.5–6.0 nm; Allen et al., 1993) and of rDNA chromatin (~4.5 nm; Martin et al., 1995). A source for a height decrease could be a coverage of the sample surface with residues from the sucrose/formaldehyde solution, which was used for centrifugation of the chromatin onto the glass substrates. Partial embedding of the nucleosomal chain in such a layer would result in the observed decrease of the height. This scenario would also explain the occasional disappearance of the linker DNA as described previously (Fritzsche et al., 1994).

A cross section through the nucleosome parallel to the substrate was used for a shape determination of the nucleosome structure. The selection of the height of the cross-sectional plane is crucial. A plane near the substrate level will be influenced by the included linker DNA as well as deposits around the edge of the nucleosome (e.g., salt residues). Deposited structures would mainly add to the diameter without significant shape changes, but the linker DNA could induce an elongation of the structure due to a long major axis consisting of the DNA structure on opposite sides of the nucleosomal core. Therefore, the section plane should be high enough to avoid artifacts caused by the mentioned factors. But there is also a need for a standard-

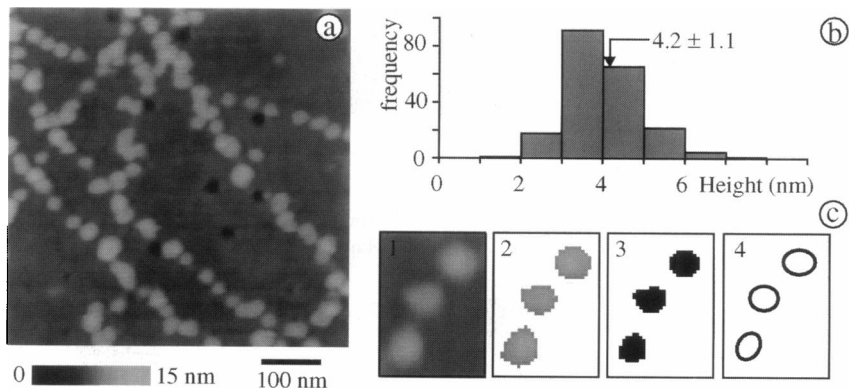

FIGURE 1 Scanning force micrograph of hypotonically spread chicken erythrocyte chromatin. The height is brightness-coded according to the gradient below the image, and the lateral scale is given by the bar of 100 nm. The "beads-on-a-string" pattern of the nucleosomal chain is clearly revealed (*a*). The nucleosome structure were selected from such samples for further processing as described in Materials and Methods. The height distribution of the selected nucleosomes is given in *b* and includes mean and standard deviation. (*c*) The steps of image processing, which starts from the original data (1). A first step is the removal of the background, yielding isolated nucleosomal structures (2). The height of the nuclesomes is determined from the highest pixel value and the average background level, and a cross section at half-maximum height results in a sectioning plane (3). This plane is described by measuring the perimeter and area, or by using the major and minor axis of a best fit ellipse (4).

ized height, avoiding any subjective influence. We chose the cross section at half-maximum height, which is easily accessible by automated image processing and well above the height of the linker DNA (<1 nm) in nucleosomal chains (Fritzsche et al., 1994). A comparison of a section near the substrate and at half-maximum nucleosome height typically yields an irregular shape for the lower section and a more well-defined ellipsoid shape of smaller size for the higher section (Fritzsche and Henderson, 1996a). The applied procedure of extracting a cross-sectional plane from the three-dimensional image demonstrates the advantage of SFM. Separation of structural features in the nanometer range from the background noise is straightforward and allows a more comprehensive characterization of small biomolecules.

The cross section near the substrate (1.3 nm above the average substrate level) yielded areas with two axes of different lengths, as demonstrated by the distribution function of the major and minor axes in Fig. 2 *a*. The mean values differ by more than 20 nm. Fig. 2 *b* shows a major: minor axis histogram of the values from Fig. 2 *a*, with a median at 1.27 ± 0.21.

The cross section at half-maximum height results in sharper peaks for the distribution of the lengths for the major and minor axes (Fig. 2 *c*) compared to the cross section near the substrate. Both axis lengths decrease from the lower cross section to values of 14.7 ± 3.5 nm (minor) and 21.1 ± 5.1 nm (major), respectively. The resulting distribution of the major: minor axis ratio is given in Fig. 2 *d*. Neither diagram showing the ratio of the major to the minor axis (Fig. 2, *b* and *d*) gives any indication for another maximum, and the measured distributions are significantly different from the expected value of 1 for a circular structure.

Scanning force microscopy is based on sensing the surface topography by a sharp tip. If the tip dimensions are in the range of the imaged features as in the case of the nucleosome study presented here, the visualization process is influenced by a convolution of the tip geometry and sample. This effect results in a broadening of steep surface features due to an edge contact of the scanning tip. For tips with a mainly spherical shape, the broadening occurs in all lateral directions, but in the case of a deformed tip a deformation of the sample image occurs. Such a deformation would interfere with geometrical investigations; therefore we tested for this possibility by determining the angle of the major axis of the inscribed ellipse. No preferred orientation was found, and observed differences compared to a random distribution could be explained by orientation of the nucleosomal fibers (manuscript in preparation). In control experiments we determined the angle distribution from samples with obvious tip artifacts and found sharp maxima. Therefore we exclude the possibility that the nucleosome shapes observed were derived primarily from the tip shape. Thus, to overcome difficulties due to the broadening effect of the

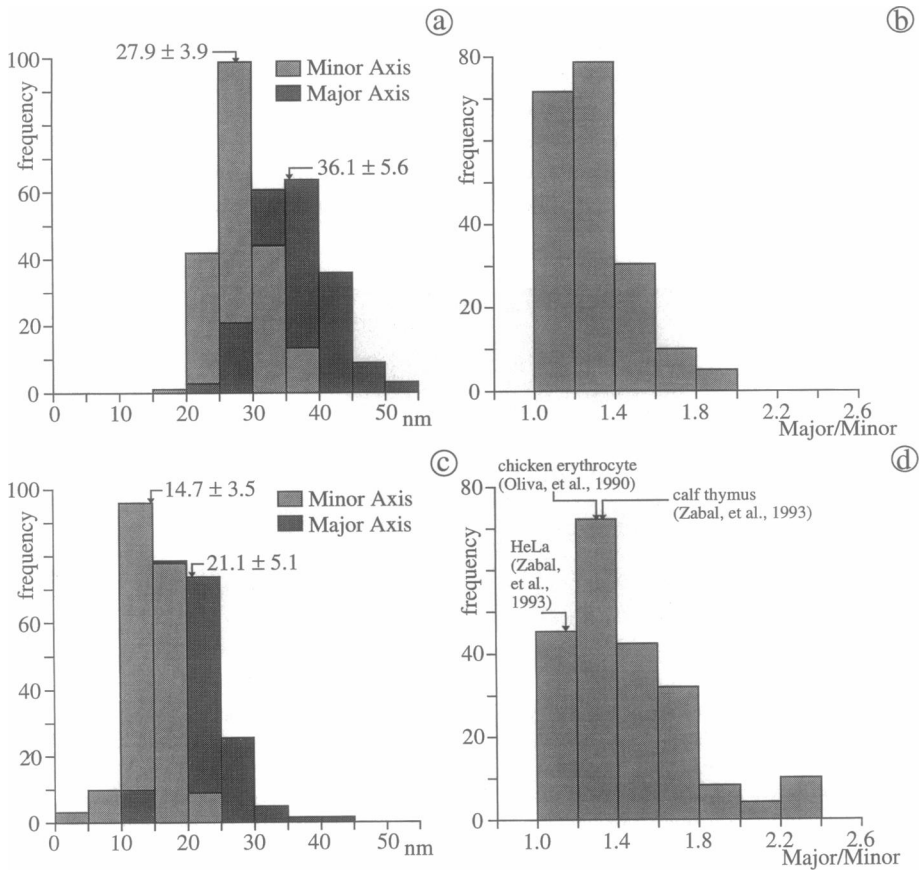

FIGURE 2 Values for the major and minor axes and the resulting ratio (major:minor) for the inscribed ellipses for a cross section near the substrate level (*a*, *b*) and at half-maximum height (*c*, *d*). The values for the median and the standard deviation for the axis values are given in the graphs. For comparison literature values are inserted in *d*.

tip, we use only the ratio of the length of the major and minor axes. This ratio is hardly influenced by the tip geometry if we assume a spherical tip.

Several methods are available to describe the shape of features based on feature dimension. In the following section we apply two of them to the investigated nucleosome cross sections: 1) the form factor = 4 * Π area/perimeter^2, and 2) the aspect ratio = major axis:minor axis (Russ, 1989). For a better understanding of the meaning of these parameters, we use geometrical figures as simplified models for the shape of the cross sections. An ellipse with different ratios of major and minor axis is shown in Fig. 3 *a*. The first ellipse (a1) with a ratio of 1 is actually a circle, and this shape results in a form factor of 1.0 (Fig. 3 *d*, upper row) and an aspect ratio of 1.0 (Fig. 3 *e*, upper row). With increasing deformation of the circle (a1 to a4) the form factor decreases, to finally reach a value of 0.34 for an ellipse with an ratio of major:minor axis of 10 (a4). The aspect ratio increases with the deformation of the circle; the value for the last ellipse (a4) is 10, far outside the range shown.

A comparison of the values from simulated shapes and the experimentally measured data results in different models for the two parameters. A comparison with the experimentally measured form factors (bars in Fig. 3 *d*) yields the value for ellipse a3 as nearest to the experimental median, but the aspect ratio of the experimental values lies between the aspect ratios of a1 and a2.

These differences point to significant differences between the real and the elliptical modeled shapes. We therefore used another set of simulated shapes, starting with an ellipse (b1), and cutting partially the area by preservation of the major and minor axis (b2, b3), finally ending in a cross (b4). This procedure changes the ratio between area and perimeter by decreasing the area faster than the perimeter; therefore the form factor decreases from 0.77 (b1) down to 0.04 (b4). The increasing values of the aspect ratio for the simulations b1-4 illustrate that the aspect ratio is based on the best fit ellipse and not the greatest dimensions (which are constant). To demonstrate the procedure used in National Institutes of Health Image, the resulting ellipse (gray) is overlayed on the simulated shapes (Fig. 3 *b*, right column). The comparison with the experimental data shows that, in view of the form factor, the ellipse b1 is the best description, which is not in agreement with the aspect ratio determination. None of the aspect ratios of the simulation approached that of the experimental data, indicating a need for additional improvements in this model. This can be explained by two factors that influence the image of the nucleosomes. The first is a flattening and partial collapse due to dehydration, which smoothes sharp corrugations; the second is the convolution of tip and sample geometry, basically with a similar result. This explanation was tested with another set of simulated shapes in which an ellipse (c1) was gradually eroded by removing pixels from the edge (c2-4). The form factors of the pixelwise eroded shapes

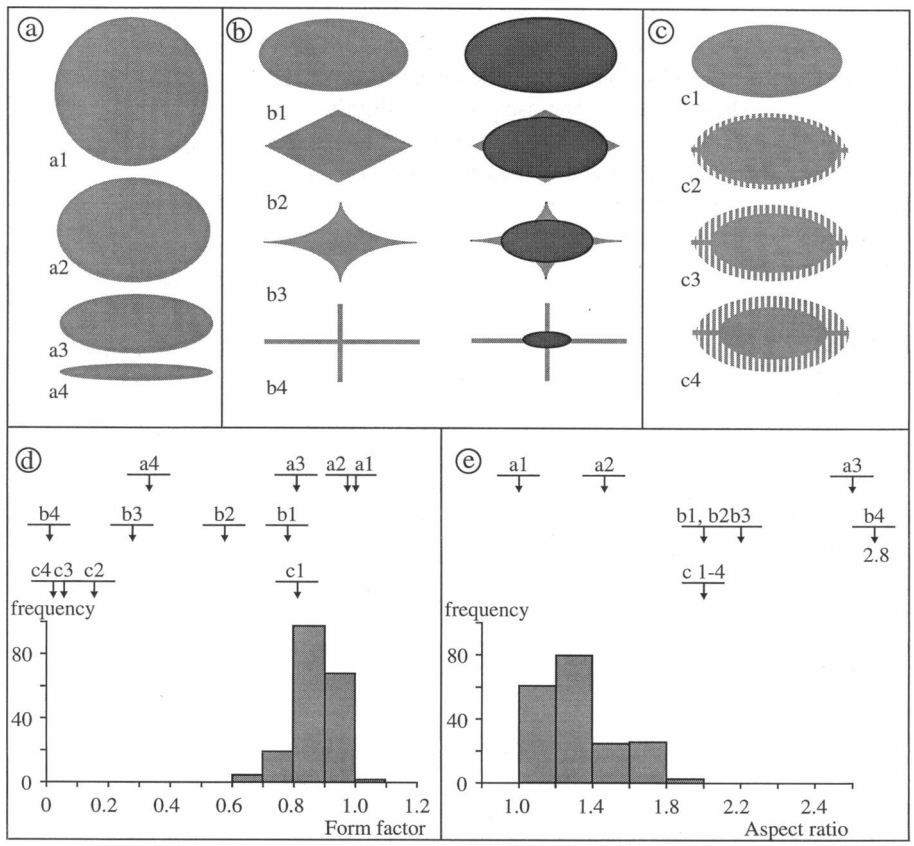

FIGURE 3 Geometrical description using form factor (4 * Π * area/perimeter^2) and aspect ratio (major/minor axis). (*a*) Ellipses with a axis ratio of 1:1 (a1), 1.5 (a2), 2.5 (a3), and 10 (a4). (*b*) Geometrical figures derived from an ellipse (b1) by cutting the area but preserving the inherent axis (b2, b3) down to a cross (b4). To visualize the work of the image processing, the best inscribed ellipse is overlayed (right column). (*c*) Geometrical figures derived from an ellipse (c1) by pixelwise removal of area (c2-4). (*d, e*) Distribution of the form factors and the aspect ratio for the nucleosome section at half-maximum height; the values for the figures from *a*–*c* are also included.

were all below 0.2 and therefore far from the experimental value of ~0.9; only the complete ellipse c1 exhibits a value in the experimental range. The erosion shapes all had the same aspect ratio, which is the value of the starting shape.

Summing up the results from the simulation, the most probable shape for the nucleosomes is an ellipse with an aspect ratio at 1.2–1.4, without cut regions, and with a relatively smooth perimeter.

A comparison of the measured aspect ratio distribution function with literature values is shown in Fig. 2 *d*. The measured aspect ratio of chicken erythrocyte nucleosomes peaks at ~1.3. This value confirms results from electron spectroscopic imaging of nucleosomes from the same source (Oliva et al., 1990) and is flanked by values determined for HeLa and calf thymus nucleosomes (Zabal et al., 1993).

An investigation of the salt dependence of the nucleosome elongation was hampered by the condensation of the nucleosomal fiber in an environment with higher salt concentrations (Fritzsche et al., 1995a). Studies are under way to determine the distribution of single nucleosomes in the complex fiber structure, but overlaying structures cannot be fully resolved, because of the inherent limitation of SFM as a profilometric method.

The determined aspect ratio of ~1.30 is comparable to values determined for chicken erythrocyte nucleosomes by electron spectroscopic imaging (1.30; Oliva et al., 1990). It was suggested that the elongation of adsorbed nucleosomes is due to substrate-nucleosome interactions, which result in structural changes compared to the structure of nucleosomes in solution. In particular, the binding of nucleosomal cores to positively charged EM support films resulted in a destabilization based on competition between the support and the histones for DNA binding (Oliva et al., 1990). In our study the nucleosomal chain was bound to a glass substrate. The use of glass substrates for chromatin (Schlammadinger, 1990) or metaphase chromosome (Harrison et al., 1981) preparations uses the high affinity of glass surfaces for DNA-protein complexes, which could affect the structure of the adsorbed nucleosomes by the aforementioned competitive binding.

CONCLUSION

The study demonstrates the successful application of scanning force microscopy for conformational investigations of biomolecules in the nanometer range, namely, nucleosomes. Cross sections of structures in this size range are hardly accessible by conventional 3-D reconstruction methods because of the size range or overlaying background noise in the images. The applied algorithm shows the potential to eliminate the influence of tip geometry by using relative parameters such as axis ratios. Further investigations are aimed toward a possible alignment of the core particles along the nucleosomal chain axis and the use of volume information for the characterization of small biomolecules.

We thank S. Schaus for careful reading of the manuscript. WF would like to thank H. Spring for his introduction to the sample preparation technique.

This work was supported by the German Academic Exchange Service. This is journal paper no. J-17021 of the Iowa Agriculture and Home Economics Experiment Station, Ames, IA, project no. 3064.

REFERENCES

Allen, M. J., X. F. Dong, T. E. O'Neill, P. Yau, S. C. Kowalczykowski, J. Gatewood, R. Balhorn, and E. M. Bradbury. 1993. Atomic force microscope measurements of nucleosome cores assembled along defined DNA sequences. *Biochemistry*. 32:8390–8396.

Bustamante, C., D. A. Erie, and D. Keller. 1994. Biochemical and structural applications of scanning force microscopy. *Curr. Opin. Struct. Biol.* 4:750–760.

Fritzsche, W., and E. Henderson. 1996a. Ultrastructural characterization of chicken erythrocyte nucleosomes by scanning force microscopy. *Scanning*. 18:138–139.

Fritzsche, W., and E. Henderson. 1996b. Volume determination of human metaphase chromosomes by scanning force microscopy. *Scanning Microsc.* In press.

Fritzsche, W., A. Schaper, and T. M. Jovin. 1994. Probing chromatin structure with the scanning force microscope. *Chromosoma*. 103: 231–236.

Fritzsche, W., A. Schaper, and T. M. Jovin. 1995a. Scanning force microscopy of chromatin fibers in air and in liquid. *Scanning*. 17:148–155.

Fritzsche, W., J. Vesenka, and E. Henderson. 1995b. Scanning force microscopy of chromatin. *Scanning Microsc.* 9:729–739.

Hansma, H. G., and J. Hoh. 1994. Biomolecular imaging with the atomic force microscope. *Annu. Rev. Biophys. Biomol. Struct.* 23:115–39.

Harauz, G., and F. P. Ottensmeyer. 1984. Nucleosome reconstruction via phosphorus mapping. *Science*. 226:936–940.

Harrison, C. J., M. Britch, T. D. Allen, and R. Harris. 1981. Scanning electron microscopy of the G-banded human karyotype. *Exp. Cell Res.* 134:141–153.

Libertini, L. J., and E. W. Small. 1982. Effects of pH on low-salt transition of chromatin core particles. *Biochemistry*. 21:3327–3334.

Lyubchenko, Y. L., B. L. Jacobs, S. M. Lindsay, and A. Stasiak. 1995. Atomic force microscopy of nucleoprotein complexes. *Scanning Microsc.* 9:705–727.

Martin, L. D., J. P. Vesenka, E. Henderson, and D. L. Dobbs. 1995. Visualization of nucleosomal structure in native chromatin by atomic force microscopy. *Biochemistry*. 34:4610–4616.

Oliva, R., D. P. Bazett-Jones, L. Locklear, and G. H. Dixon. 1990. Histone hyperacetylation can induce unfolding of the nucleosome core particle. *Nucleic Acids Res.* 18:2739–2747.

Richmond, T. J., J. T. Finch, B. Rushton, D. Rhodes, and A. Klug. 1984. Structure of the nucleosome core particle at 7 Å resolution. *Nature*. 311:532–537.

Russ, J. C. 1989. Automatic methods for the measurement of curvature of lines, features, and feature alignment in images. *J. Comput. Assist. Microsc.* 1:39–77.

Russ, J. C. 1992. The Image Processing Handbook. CRC Press, Boca Raton, FL.

Schlammadinger, J. 1990. Immunofluorescence detection of nuclear antigens in supramolecular chromatin spread. *Methods Mol. Cell. Biol.* 1:235–241.

Sterner, R., L. C. Boffa, T. A. Chen, and V. G. Allfrey. 1987. Cell cycle-dependent changes in conformation and composition of nucleosomes containing human histone gene sequences. *Nucleic Acids Res.* 15:4375–4391.

Trendelenburg, M. F., and F. Puvion-Dutilleul. 1987. Visualizing active genes. *In* Electron Microscopy in Molecular Biology. IRL Press, Oxford. 101–146.

Van Holde, K. E. 1988. Chromatin. Springer, New York.

Zabal, M. M. Z., G. J. Czarnota, D. P. Bazett-Jones, and F. P. Ottensmeyer. 1993. Conformational characterization of nucleosomes by principal component analysis of their electron micrographs. *J. Microsc.* 172:204–214.

Zentgraf, H., U. Müller, and W. W. Franke. 1980. Reversible in vitro packing of nucleosomal filaments into globular supranucleosomal units of whole chicken erythrocyte nuclei. *Eur. J. Cell Biol.* 23: 171–188.